The use of Rapid Prototyping techniques (RPT) to manufacture Micro channels suitable for high operation pressures and µPIV

1. Abstract

The use of microfluidics is extensively related to bioapplications where the devices normally actuate at atmospheric pressures. The advantages of miniaturization are also valuable in many industrial applications, but building microfluidic circuits that withstand high pressures is still a challenge. This paper presents a new methodology to manufacture micro-channels suitable for high operating pressures and micro Particle Image Velocimetry measurements using a rapid-prototyping high-resolution 3D printer. This methodology can fabricate channels down to 250 µm and withstand pressures of up to 5 ± 0.2 MPa. The manufacturing times are much shorter than in soft lithography processes since there is no need to create a mold and the material can be chosen from a range of different UV curable resins that present a Young Modulus ranging from 2000 to 3000 MPa.

2. Introduction

Current research in the field of microfluidics using micro Particle Image Velocimetry (µPIV) covers investigations of the fundamental flow properties of e.g. complex fluids like grease (Green et al., 2011; Li et al., 2013; Li et al., 2012; Baart et al., 2011; Westerberg et al., 2010) or flow in medical devices (Madadi et al., 2013; Lewpiriyawong et al., 2008). The method used to manufacture the channels depends on its dimensions where, in the case of devices of the order of 1 mm in size, conventional manufacturing processes such as chip removal or electrical discharge machining are commonly used, while for channels with smaller dimensions, different micro-fabrication techniques have proven more suitable (Brittain et al., 1998, Weibel et al., 2007). Weibel et al., 2007 showed that for the micro-scale channels the typical manufacturing technique is soft lithography (Armani et al., 1999) where the base material is polydimethylsiloxane (PDMS), or some other polymer with similar characteristics. This polymer has a low Young Modulus (360-870 kPa), implying it can be easily deformed and 3D structures are not easily manufactured. There is a clear need of a straight forward manufacturing technique that provides the finished part from the AUTOCAD drawing, for instance Wu et al., 2011 proposed to use a high accuracy positioning table with a novel ink which allowed the direct fabrication of micro-channels.

Many engineering applications operate under elevated pressures as illustrated by Egham, 2006, who used an oleo-hydraulic pump that operated up to about 500 atmospheres, and Sanches et al., 2013 showing oil distributors or new flushing bearings methods operating at up to 60 MPa. In most of these devices there are micro-channels where grease and/or oil flows, and the behavior of the lubrication materials in these channels can modify the expected life of all actual components. It is of great interest and importance to analyze the flow behavior of greases in channels dimensioned in the micron range in order to be able to optimize the lubrication of the actual component. However, conventional micro-manufacturing processes such as soft lithography or Reactive Ion Etching (RIE) on silicon or glass (Ciftlik et al., 2012) have shown different challenges when operating at high pressures. PDMS channels are manufactured using soft lithography, where the pressure influences the channel deformation which in turn leads to experimental results far removed from realistic values (Gervais et al., 2006; Hardy et al., 2009), unless the channels are modified by adding other materials such as glass to make them more rigid (Inglis et al., 2010) or layer of UV-curable thiolene resins (Madadi et al., 2013). This reason has motivated the use of other technologies to manufacture the micro-channels, such as RIE or Electric Discharge Machining (EDM). RIE is normally used for

brittle materials (silicon or glass) which can easily break if they suffer an impact, and EDM has been shown to work on channels down to 500 μm (Sultan et al., 2012), but the main problem was the grease leakages through the joint of the plates and the micro-channel size limit.

Previous micromachining processes such as soft lithography, RIE, and EDM have shown different challenges when operating at high pressures. Either the low Young Modulus of PDMS causes elastic deformation of the channels which in turn affect the agreement between the experimental results and the expected results, or the number of manufacturing steps is increased. Moreover, the interconnections with external pipes and pumps are difficult to integrate in all the aforementioned processes. The novel manufacturing method presented in this paper can thanks to the use of a high resolution 3D printer with a wide material range (Young Modulus from 2000 to 3000 MPa) produce micro-channels that can operate at high pressures and also have integrated hose connections to pipes and pumps. In precise machining technologies such as Electric Discharge Machining (EDM) it is extremely difficult to machine accurately channels smaller than 500 μm. In previous studies (Li et al., 2012; Baart et al., 2011; Westerberg et al., 2010) this methodology was used but the main problem was the grease leakages through the joint of the plates and the micro-channel size limit.

The recent improvement in 3D printer resolution has made 3D printers a viable alternative for machining microfluidic circuits. Here polyjet technology has made it possible to manufacture faster and cheaper than EDM. Bonyar et al., 2010 used this technology to manufacture molds used in soft lithography to build PDMS micro-channels, substituting the lithography step used on another photopolymer called SU8. According to Bonyar et al., 2012, 3D-printed molds could be manufactured much faster than conventional ones. However, focusing on the accuracy of the printed parts it was concluded that the accuracy is higher for the glossy printing mode (resulting in a glossy surface finish) compared to the corresponding matt mode. A disadvantage with the glossy mode however, is an induced channel widening due to the leaning of the photopolymer material after deposition, which limits the achievable channel dimensions (Bonyar et al., 2012).
In their study, Bonyár et al., 2012 always used the 3D printer for mold manufacturing but they never used it for micro-channel manufacturing.

In this paper, we propose a novel manufacturing technique based on building the micro-channels by using a 3D printer directly and then sealing them using glass slides and ultra violet (UV) curable glue. The main advantages of this system are that it is faster than the current technologies and it is more cost-effective. Furthermore, it is possible to build micro-channels that withstand high pressures without the elastic deformations that other common micro-manufacturing materials such as PDMS suffer.

3. Materials and methods

The novel manufacturing method developed takes advantage of the recently improved resolution in 3D printers to manufacture a RPT part that contains the hose connections and a micro-channel useful for microfluidics. In this section a method to assemble one wall of the micro-channel using UV curable glue with a glass slide is presented – an operation required to prepare the channel for μPIV measurements.

3.1 Materials

The materials used to perform the channel construction and flow measurements are listed below.

- Microscope glass slide of dimensions 76 x 26 x 1 mm according to ISO 8037-1:1986.
- Standard hydraulic hose from Lincoln Industrial Corp., model WEDK4-M6x1. 4 mm diameter tube and M6 x 1 metric thread.
- 31G syringe type (0.25 mm diameter needle).
- UV curable glue (Delo-photobond GB368 curing from 320 till 420 nm). The curing time is 15 s at 55 mW/ cm^2.
- 3D Printing Object 30 Printer from Stratasys using VeroWhitePlus RGD835 modelling material and FullCure 705 support material. The resolution of the printer is 600 dpi (42 µm), 600 dpi (42 µm) and 900 dpi (34 µm) in the x, y and z-axis respectively according to its datasheet. All fabricated structures were first cleaned with pressurized water and subsequently submerged in a 4% NaOH solution for 15 minutes. SolidWorks 2012 was used for designing the objects and STL format was used to export the file to the 3D printer.
- Grease pump from Lincoln Industrial Corp. model QLS 401 - 230VAC. The minimum flow rate in a single output is 0.2 cm^3 and the pressure relief valve actuates at 20.5 MPa.
- Ø6 x 1.5 pressure plastic tube 7.5 MPa at 20ºC (with triple safety) from the manufacturer Lincoln Industrial
- 6 ± 0.1 MPa manometer.
- Polytetrafluoroethylene (PTFE) used at the manometer and hydraulic hose threads.
- Syringe pump KDS410 from KD Scientific.
- Laser from Litron Lasers, model LDY301-PIV.
- Microscope from Leica, model 090-135.003 with 20X objective.
- Software DynamicStudio version 3.40.82 from Dantec Dynamics.
- Micro-particles type MF-Rhodamine B particles with a diameter of 3.23 µm ± 0.06 µm.
- Lithium grease, NLGI grade 1.
- 20 ml syringe.
- Sensofar, microscope confocal model PLu neox with 10X objective.
- Software SensoSCAN version 3.3.1 from Sensofar.

3.2 Methods

In the present study a Rapid Prototyping Printer (RPT) from Stratasys, model Object 30, is considered to directly print channels 250 µm wide and 250 µm thick using VeroWhitePlus, which is a rigid thermoplastic of acrylic type, and microscope glass slides to close the channel configuration. The attachment of both parts will be done using UV curable glue.

The use of RPT allows integration of the connection in the same part where the channel is created. Figure 1a shows an example of the RPT part together with the glass-bottomed part (enclosure) to make µPIV measurements possible. The part manufactured by RPT embeds the micro-channels and the standard hydraulic hose to connect the inlet pipe.

A detail of the RPT part directly manufactured by the printer is shown in figure 1b and figure 1c. Here subfigure 1b shows the top view of the part containing the channel inlet and outlet. Figure 1c is the corresponding bottom view of the part, where two details are emphasized: four centering columns that help during the bonding procedure and an embedded seal around the channel to

prevent the channel from clogging when fixing the glass plate using a UV curable adhesive. The four columns and the seal are the same height.

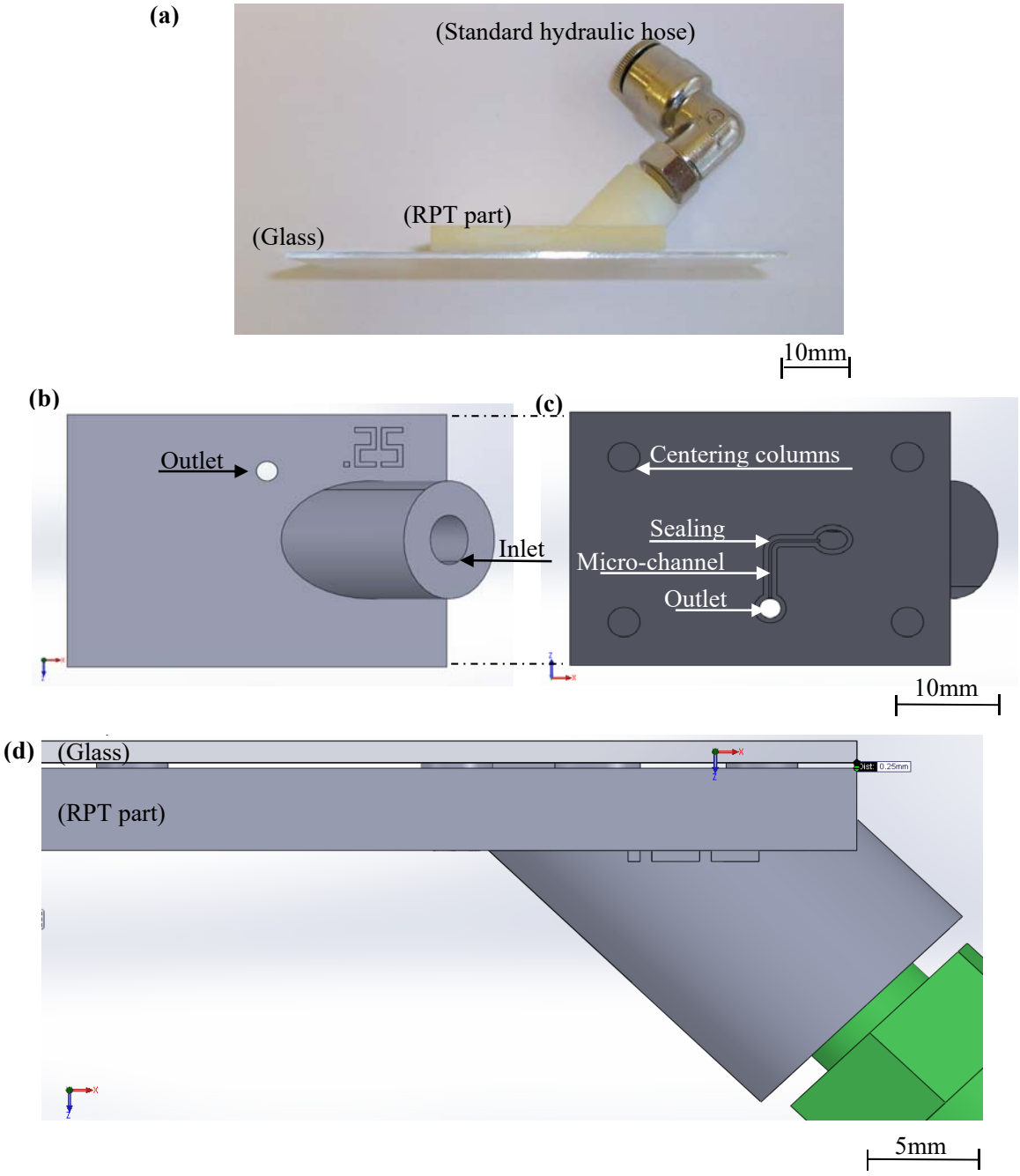

Figure 1. (a) View of the micro-channel assembly. (b) RPT part top view and (c) RPT part bottom view. (d) Assembly detail of the gap between the RPT part and the glass.

The micro-channel and the connection to the hydraulic hose have been manufactured as a single, integrated part using the 3D printer; see figure 1b and figure 1c. The 3D printer has two different surface finishes: firstly a glossy finish having a surface roughness (Ra-value) of the order of 10 nm and secondly a matt finish having a Ra-value of the order of 1.5 µm. According to Bonyár et al., 2012 the glossy surface finish distorts the final dimensions of the channel, which would consequently generate more reflections during µPIV measurements (Stanislas et al., 2003). Therefore a matt surface finish has been considered.

Once the actual part has been printed, the support material is removed using pressurized water and the thread to connect the hydraulic hose is hand-tapped. The RPT part is then first submerged in a 4% NaOH solution for 15 minutes and thereafter in de-ionized water for 15 minutes. To seal the top surface of the micro-channel, standard glass slides with a dimension of 26 mm x 76 mm x 1 mm are used; see figure 2a-b. In order to withstand the high pressure, the glass is bonded to the RPT part using a flexible UV curable adhesive labeled Delo-photobond GB368. Before the bonding procedure all the parts are cleaned and compressed air is used to dry the RPT part. To clean the glass substrate, it is submerged in acetone for 10 min. and methanol for 10 min. respectively. Subsequently, it is boiled in a piranha solution (H_2SO_4:H_2O_2 = 3:1) for 15 min. The slides are then immersed in de-ionized water for 5 min. and dried using nitrogen gas. Finally, the cleaned glass substrates are placed in a conventional oven for 20 min. at 85 ºC and after that dried using compressed air.

To start the bonding procedure two glue drops are placed near the columns in order to hold the glass in place and mechanical pressure is applied to ensure good contact (figure 2a), whereafter a first UV curing is carried out; see figure 2b. Then the gap between the glass and the surface of the RPT part is filled with glue using a syringe of type 31G (needle Ø 0.25 mm); see figure 2c. This step is critical because if the glue arrives at the seal and it is not cured fast enough it can fill the channel due to the generated capillarity forces. Finally the part is placed under the UV exposure lamp just when the glue is near the seal; see figure 2d. After the perimeter of the channel is sealed, the rest of the surface is filled with glue in order to distribute the pressure uniformly during working conditions.

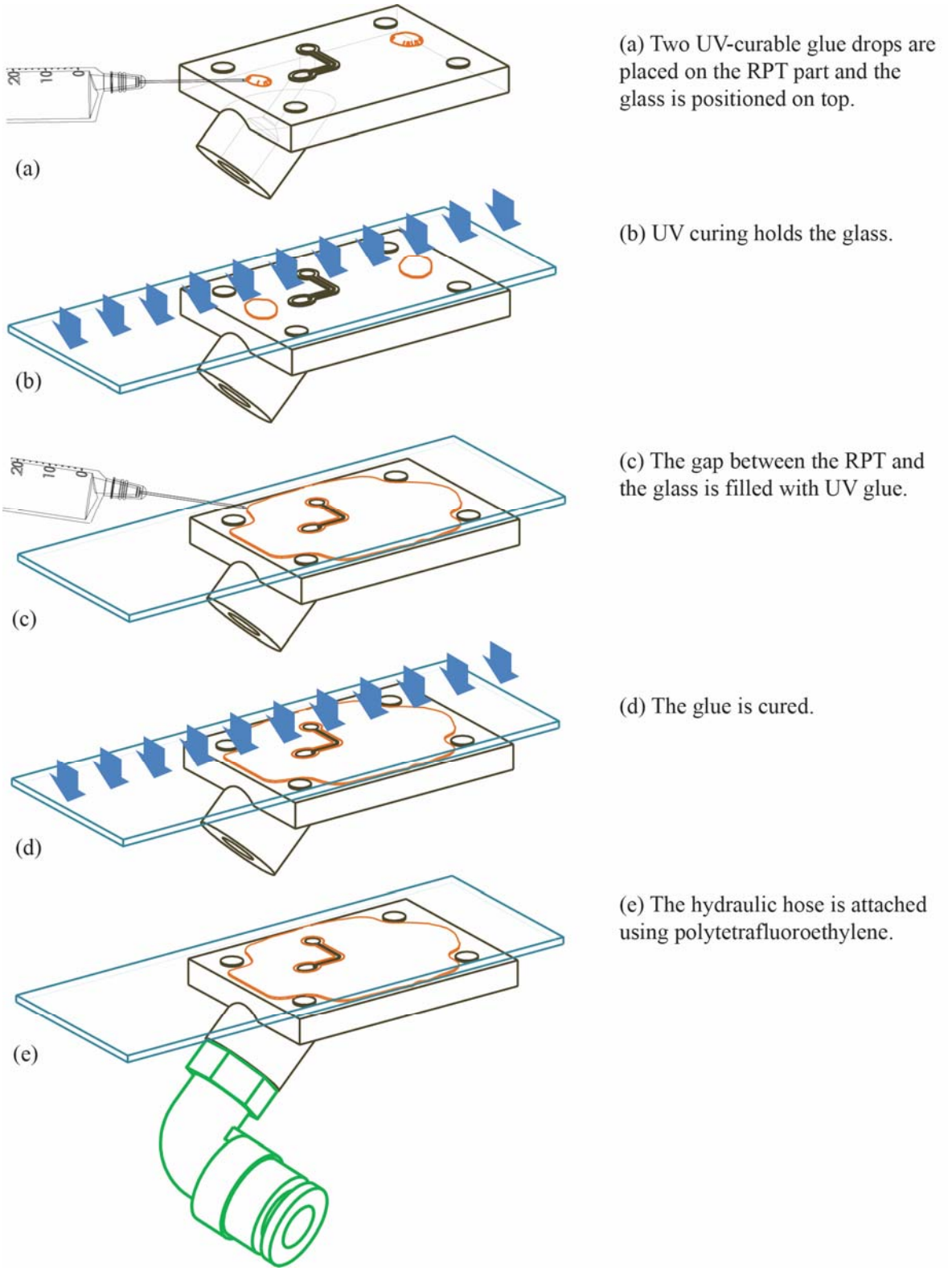

Figure 2. Fabrication steps of micro-channels suitable for high operating pressures and μPIV measurements.

4. Experiments

To verify the quality of the RPT micro-channels and the possibility to use them in high-pressure µPIV measurements, two parameters are evaluated: firstly the maximum pressure without leakages at the channels, and secondly the channel transparency without µPIV reflections. To evaluate these parameters, two experimental setups are prepared. In figure 3 the experimental setup to determine the maximum pressure without leakages at the channels is presented. Here the RPT part was specially designed to connect a manometer at the outlet measuring the pressure at the end of the micro-channel. The obtained value is compared to the pump manometer to verify that the pressure is transmitted along the grease circuit and to measure the pressure losses in the pipe connecting the grease pump outlet with the micro-channel. The pump is set for manual injection of the grease and when the manual injection button is pulsed, the grease pump will inject 0.2 cm^3 of grease in the circuit shown in figure 3. So at the beginning of the experiment, the grease circuit is filled using the manual button without the manometer at the outlet. When there is grease flow at the outlet, the manometer is connected to close the circuit. The pressure difference between the inlet and outlet is 0.2 MPa at 20 ºC.

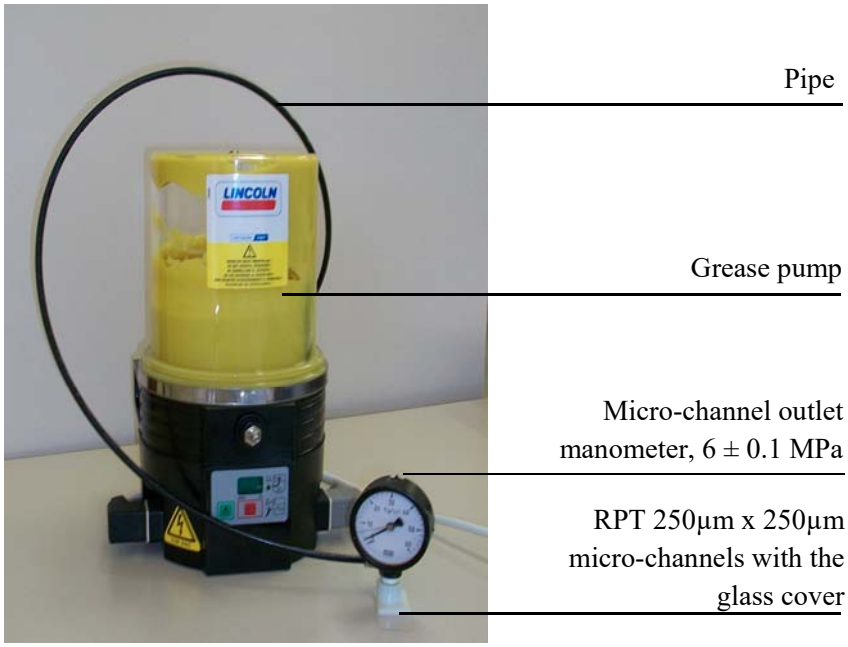

Figure 3: Experimental setup to determine the maximum pressure without leakages and fractures at the channel structure.

In order to reach the maximum pressure, the amount of grease is increased manually using the greasing button on the grease pump. The procedure to obtain the maximum pressure is as follows: inject grease, wait until the pressure difference between the pump manometer and the channel outlet manometer is 0.2 MPa, and when the pressure remains unchanged for 10 minutes proceed to inject grease using the manual greasing button. The detection of leakage is then ocular, done by monitoring the outlet manometer pressure.

Figure 4 shows the experimental setup used to validate the manufacturing technology with respect to µPIV characterization. The main principle behind PIV is to take pictures of a particle-seeded material (fluid); grease in this case. The light source is a doubled-pulsed laser enabling a series of double-framed pictures separated by a given time difference. PIV is non-intrusive meaning no probes have to be inserted into the fluid to perform the measurements – hence avoiding the possible problem of an inserted object perturbing the flow motion. The method is also indirect as the analysis is performed on the motion of the seeded particles – which in turn makes it crucial that the particles follow the flow motion. Suitable particles are chosen with background to the fluid density and the required light signal to be obtained. The motion of the particles is tracked using Fast Fourier Transform (FFT) and a correlation algorithm resulting in data of the fluid velocity in the actual plane of measurement. Compared to PIV in macroscopic geometries where the plane is set by a laser sheet formed by imaging optics, the plane in µPIV applications is set to the focal plane of the microscope objective as the laser light illuminates the whole volume. In the present study the tracer particles used are fluorescent MF-Rhodamine B particles having a diameter of 3.23 µm ± 0.06 µm. As shown in figure 4 the RPT part micro-channel is positioned over an inverted microscope and a high-speed camera is used to take pictures of the particle-doped grease flow.

Also, in terms of details of the micro-channel (material and manufacturing process) - which is the prime objective the present paper - it is of specific importance to have channels which prevent reflections from the laser light as these will impair the quality of the measurements.

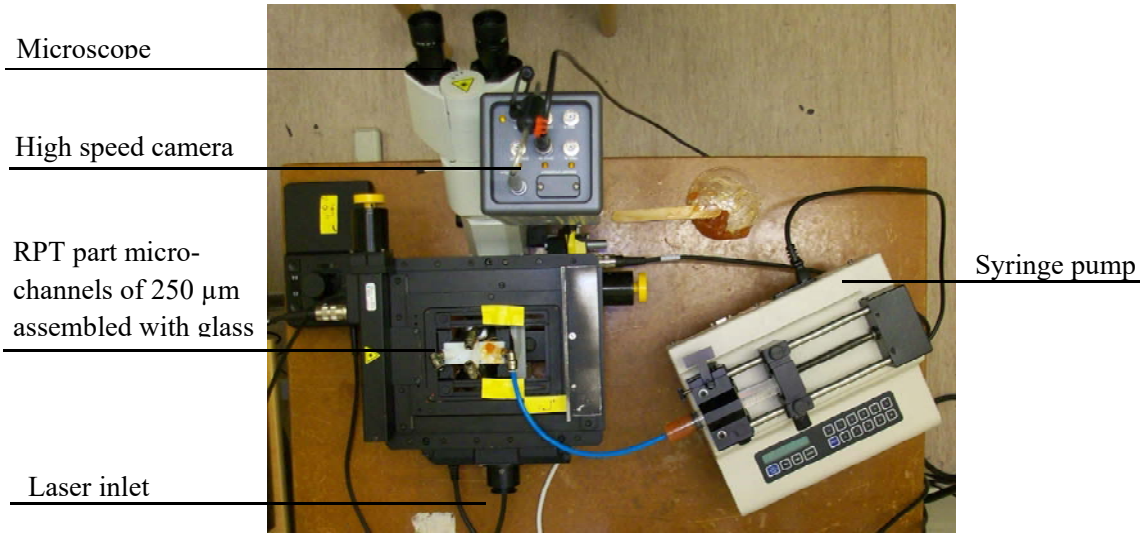

Figure 4. Setup of a µPIV experiment using an RPT part with a 250 µm square micro-channel.

The channel is validated through µPIV measurements, which test whether reflections are present, as well as monitoring the velocity distribution in the channel; see figure 5b for a measured velocity profile in the channel. This novel method investigates the possibility to continue the work in (Green et al., 2011; Li et al., 2013; Li et al., 2012; Baart et al., 2011; Westerberg et al., 2010) to also comprise high pressure flow and flow in a new set of smaller dimensions introducing shear rates being at least of an order of magnitude greater than what has been considered in the studies cited above. Based on these objectives, two flow rates were considered: a very low flow rate of 0.012 ml/

min., corresponding to a maximum velocity of the order of 0.0032 m/ s, and a higher flow rate of 0.125 ml/ min., corresponding to a maximum velocity of the order of 0.03 m/ s.

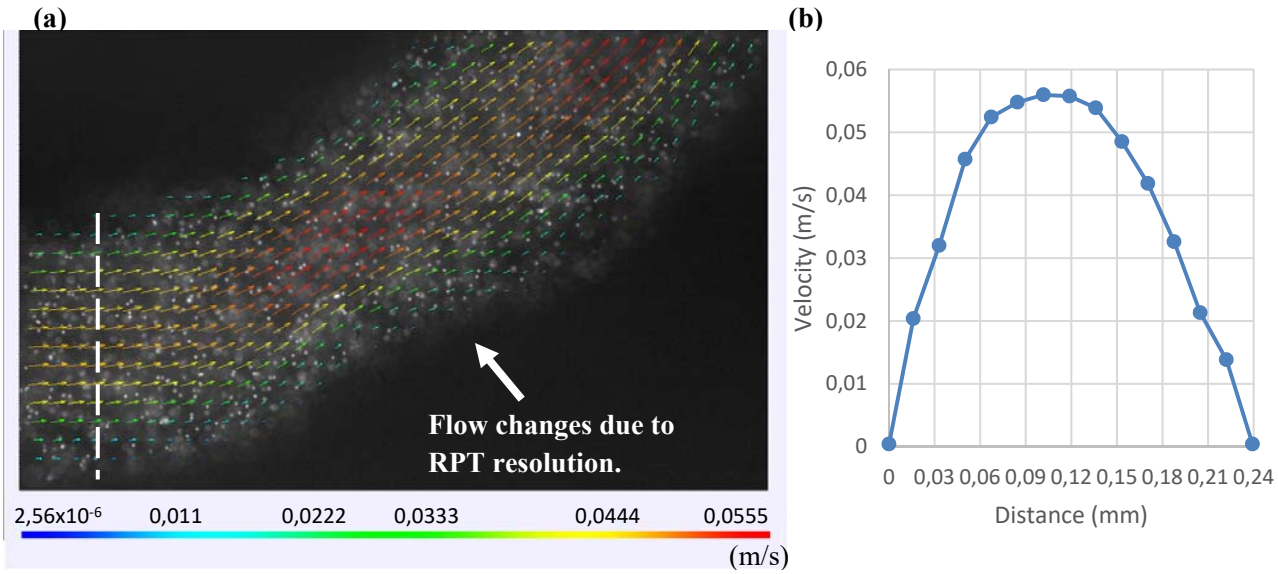

Figure 5. Flow rate of 0,125 ml/min. at straight micro-channel of 250 µm x 250 µm. (a) Microscope picture with an objective of twenty times superposed with the average vectors velocity calculated from the µPIV measurements. (b) Velocity profile at the dotted line of figure (a), the elbow entrance.

5. Results and discussion

The pressure tests were performed three times with different micro channels of 250x250 μm^2 and the results indicate that the micro channel can withstand pressures of up to 5 MPa (μ = 5 MPa, σ = 0.2 MPa) without leakages. Leakage was observed to first appear in the hose connector threads, hence indicating this to be the weakest point of whole setup. The channel material performed properly however and no cracks were observed on it.

Since the tensile strength of the glue is 20 MPa (Delo Technical Information, 2012) and the cross section of the expected channels are in the micron range (i.e. 250x250 µm), the channel- to bonding area ratio is much lower than 1 and the effect of the channel dimensions to the withstand pressure is negligible. If larger channels are required, this ratio could be increased keeping at least the ratio equal to 1.

Figure 5b shows the velocity profile at the middle of the straight inlet section of the channel (cf. Figure 1c) and figure 5a presents the velocity vector field at the elbow. The visible dots are the tracer particles in the grease. The µPIV measurements performed show that is possible to obtain high quality velocity measurements in the channel. However, some perturbations in the flow were detected close to the elbow boundaries of the channel; see figure 5a. These perturbations are caused by dimensional changes in the channel due to the printer resolution (accuracy) in the x, y, and z directions: 42 µm in x and y direction and 34 µm in the z direction respectively. In Figure 5a a

bump is visible at the lower boundary at the beginning of the elbow which causes a locally distorted flow around this region. Therefore, it is important to analyze the accuracy of the printer when manufacturing micron-sized-channels, to evaluate the limits of this novel fabrication technique.
The part shown in figure 6 has been printed to evaluate the quality of the micro channels containing elbows and/or curves, either aligned with the printer axis (bottom of the printer part) or at 45º angle (top of the printed part). Printing these geometries requires synchronization between the x- and y-axis of the printer, and always in the curved section and in the 45º channels.

The six manufactured micro channels have a square cross section with a side length ranging from 150 µm to 650 µm, with 100 µm increments. In each channel 5 different cross sections (see figure 6) were measured using confocal microscopy and since the part are thought to study tribology applications the grease intake has also been analyzed. The parts were completely submerged in grease during 7 days (168h) at 40ºC. The part weight was measured before the test and after. The weight change is summarized in

Table **1**. After the test, pressure was applied to the channels to verify that the glue withstanded the same pressure. According to the results, the parts absorbed less than 1% in weight and suffered a little change in colour.

Conditions	Not submerged, only 168h at 40ºC	Submerged with grease type NLGI-2 during 168h at 40ºC	Submerged with grease type NLGI-1 during 168h at 40ºC
Weight change	-0,11%	0,07%	0,21%

Table 1: Grease intake of VeroWhite material

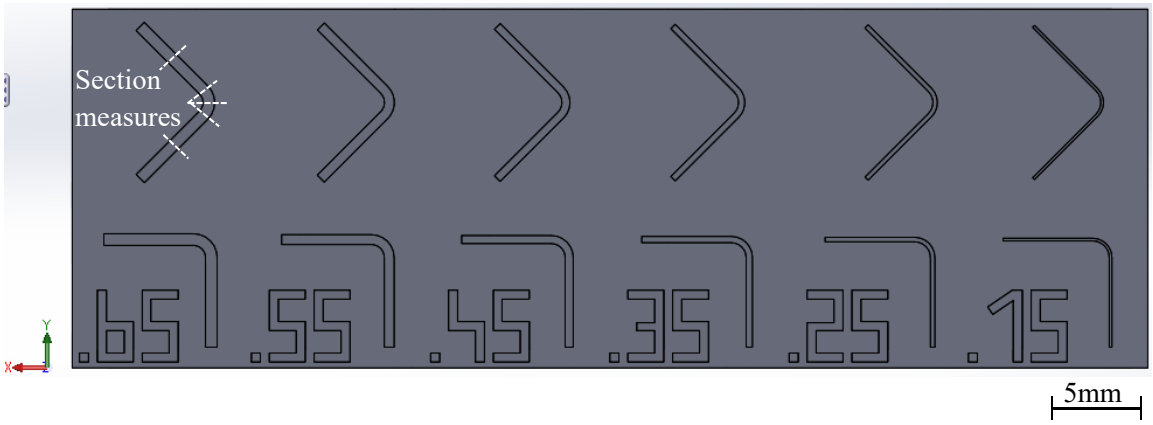

Figure 6: RPT part to evaluate the printing quality between micro channels oriented 45º to the x axis of the 3D printer and micro channels oriented in the same direction as the x-axis of the 3D printer.

Confocal microscopy provides the whole topography of the channel, see figure 7a and the topography can be analyzed at each cross-section, see figure 8. Figure 8a clearly illustrates the building process layer by layer, where we notice minimum layer thickness of resolution in z (Δz). Figure 7b plots the histogram of the different heights presents in the confocal image and we can see the two side bands around the expected height showing the effect of the resolution of the printer in some cross-sections. But the effects of the printer resolution in x and y-axis are shown in figure 7a where we can appreciate the waviness of the wall, due to the positioning precision of the laser head. As illustrated in figure 7a due to x/y resolution, the width is not constant all along the channel, causing constriction points in the x and y direction, which as a consequence narrows the channel at some locations down to 210 µm and hence affects the channel flow at the boundaries. These two effects have been analyzed the six mentioned samples and the results are summarized in figure 9 and figure 10, where the average value of channel-depth and channel-width is plotted for both cases when the printer axis are aligned with the manufactured channel and when they are tilted 45º.

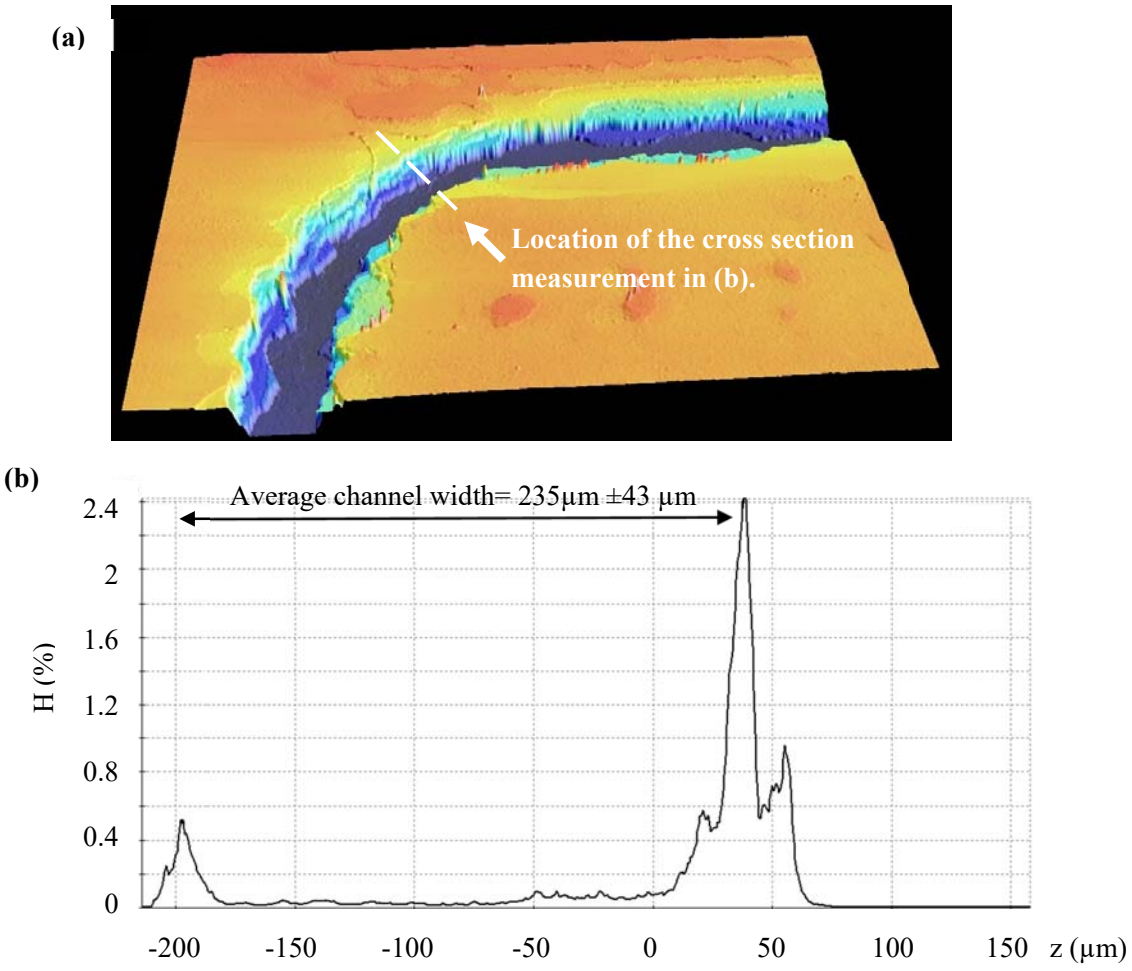

Figure 7: Microscope confocal topology analysis. (a) 3D view of the micro-channel. Figure 8 shows the cross section at the elbow. (b) Histogram of the micro-channel.

According to the results shown in Figure 9, the manufacturing depth is reliable and does not depend on the micro-channel orientation with respect to the axis of the 3D printer. In terms of the channel width accuracy/reliability, the channels tilted 45º with respect to the manufacturing axis tend to be up to 25 µm wider than the micro channels manufactured with the same x/y-axis direction. Concerning the repeatability of the channel width for the manufacturing process, it is shown that micro channels manufactured at an angle of 45º to the axis of the 3D printer have two times higher standard deviation at lower dimensions (250 µm) compared to the 650 µm width case. In terms of curvatures, even though the printer can print acute angles (< 45º), sealing this type of channels is challenging since the strong capillary flow generated in the acute angle area that can drive the glue inside the channel is clogging it. Furthermore, the current printer accuracy (42 µm in the x- and y direction and 34 µm in the z direction respectively) makes this process not feasible to manufacture channels smaller than 250 µm since the measured topography of the channels with a width of 150 µm shows that the desired width is impossible to obtain. In order to manufacture a channel using the 3D Printing Object 30, the ratio between the channel dimension and the manufacturing axis accuracy should not be less than 4.7. The required distance between channels should be in the same range (at least 200 µm) not only to ensure the channel definition but also to fill the cavities between them accurately with the UV glue and therefore provide good sealing.
This condition is illustrated when the orientation of the micro channel coincides with the x- and y-axis of the 3D printer. For this case it is shown that a micro channel up to 150 µm can be manufactured; however, the length scale of the deviation from an ideally flat wall due to the printer accuracy is of the same order of magnitude as the width of the channel, meaning the flow may be restricted at some locations in the channel. But for the case of a channel with 45° orientation, a width of 150 µm is impossible to obtain, meaning the minimum width should be 250 µm. Caution should though be considered before bonding as the channel surface at the elbow may have irregularities perturbing the flow.

Figure 8 shows two channels with a width of 250 µm. In figure 8a the channel is oriented along the manufacturing axis while in figure 8b it is tilted 45º. It is clear that the worst case in terms of the waviness of the channel wall is for the channel oriented 45° to the axis of the 3D printer. But as the dimensions are increased up to 350 µm the relative waviness improves and consequently the positive effect from tilting the channel with respect to the manufacturing axis is reduced; see figure 12 which corresponds to the 350 µm wide channel oriented 45º to the x-axis of the 3D printer.

The surface roughness measured at the bottom of the micro-channel shows that for channel sizes smaller than 250x250 µm its standard deviation increases as the micro-channel size decreases. Moreover, in micro-channels bigger than 250x250 µm the roughness is shown to not depend on the micro-channel dimension; the average Ra value is 1.87 µm and the standard deviation is 0.78 µm. Figure 11 shows the results for the Ra measurements for each micro-channel cross section.

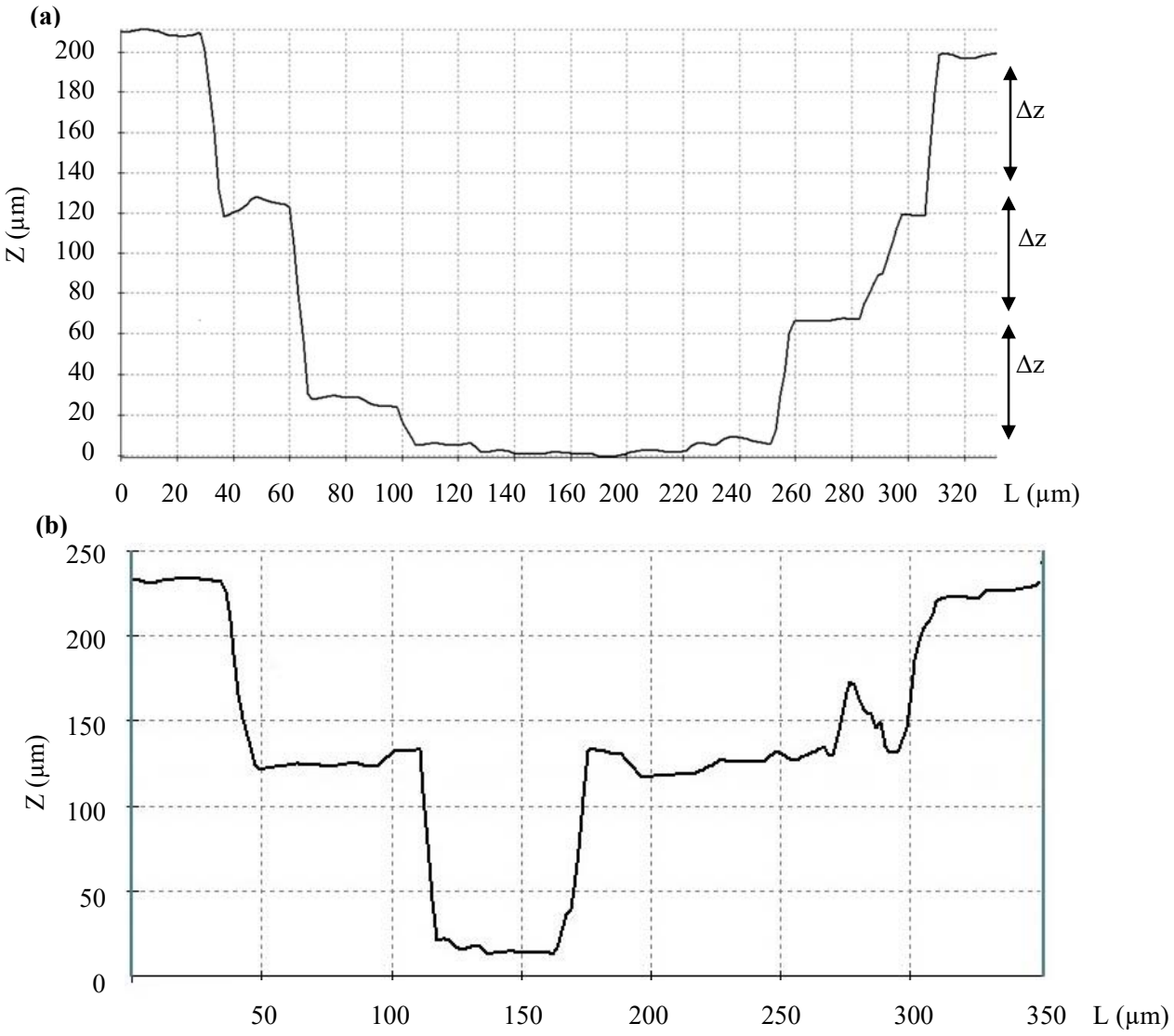

Figure 8: Cross section of the 250 µm micro channel figure 7a). (a) Printed oriented along the 3D printer manufacturing axis (b) Printed 45º to the x-axis of the 3D printer.

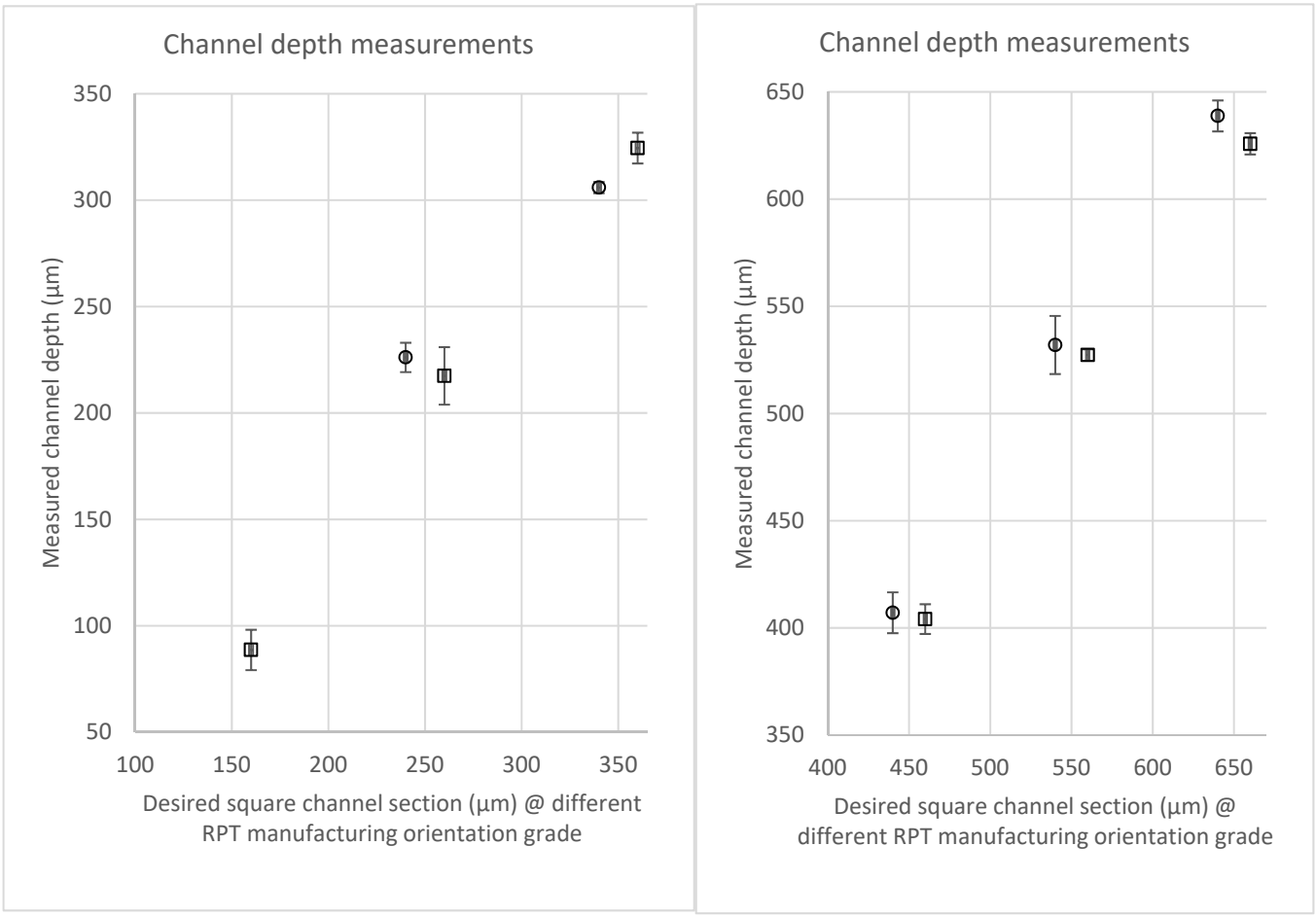

Figure 9: Channel depth measurements. The squares represent channels manufactured where the x- and y-axis coincide with the axes of the 3D printer. The circles represent the corresponding case where the channel is oriented 45º to the x-axis of the 3D printer.

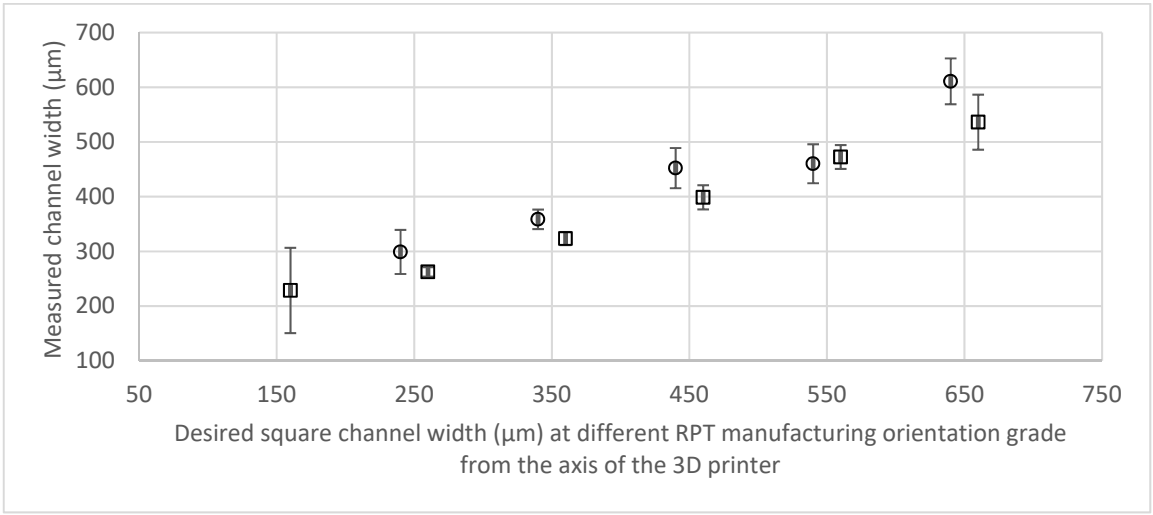

Figure 10: Channel width measurements. The squares represent channels manufactured where the x- and y-axis coincide with the axes of the 3D printer. The circles represent the corresponding case where the channel is oriented 45º to the x-axis of the 3D printer.

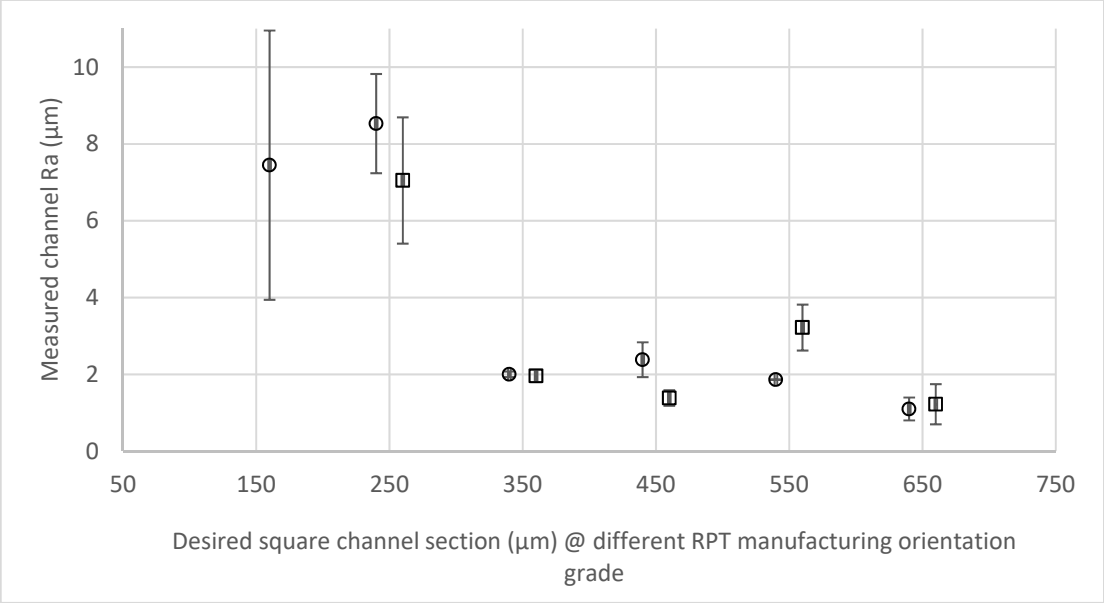

Figure 11: Channel roughness measurements. The squares represent channels manufactured where the x- and y-axis coincide with the axes of the 3D printer. The circles represent the corresponding case where the channel is oriented 45º to the x-axis of the 3D printer.

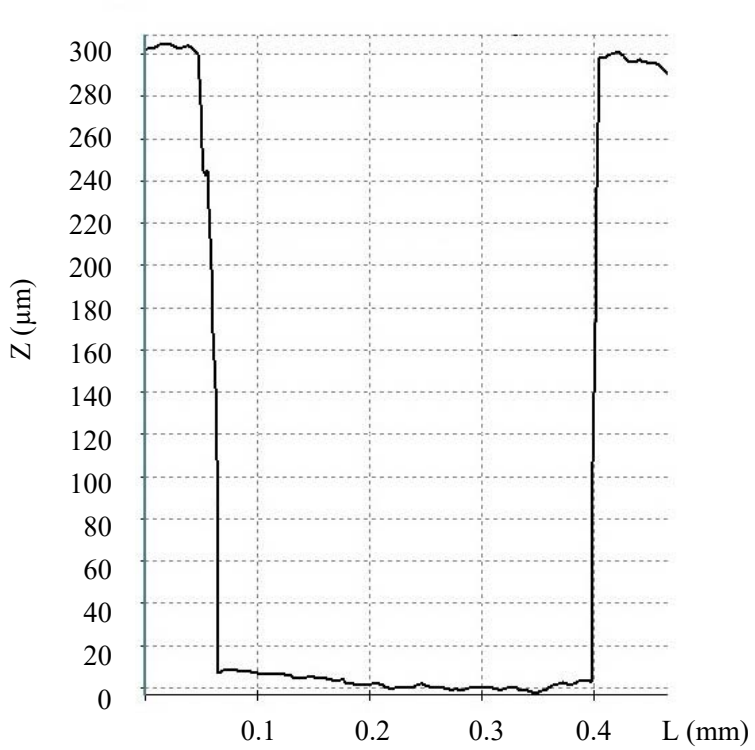

Figure 12: Cross-section of the 350 µm micro channel printed 45º to the x-axis of the 3D printer

The printer time of the RPT part used in Figure 1 is 102 minutes. This time could be minimized integrating more micro-channels in the same RPT or printing more than one RPT at the same time. The assembly time depends on the skill of the technician; for the proposed part the average time is 15 minutes. The material consumption to print the RPT parts is presented in Table 2. Therefore, the average manufacturing time and material consumption makes this process very competitive compared to previous methods using micro-fabrication technologies such as soft lithography or micro-machining.

VeroWhitePlus RGD835 consumed (1€/gr)	FullCure 705 Consumed support material. (1€/gr)	Microscope glass slides cost	UV glue cost (2€/ml)	Total cost
9gr (9€)	6gr (6€)	0.1€	0.2ml (0.4€)	15.5€

Table 2: RPT material consumption by the RPT part of Figure 1.

6. Summary and conclusions

The presented novel micro-manufacturing technique that takes advantage of RPT printing and UV curable glue opens the possibility to obtain micron-sized channels that can withstand pressures higher than 5 MPa. This manufacturing technique is much faster than previous micro-manufacturing techniques where different steps were needed to obtain the micro-machined parts. However, due to current 3D printers resolutions (around 50 µm) and according to the experimental results, channels smaller than 250 µm x 250 µm in cross-section should not be used to characterize fluid flow behaviors using micro Particle Image Velocimetry, since inaccuracies in the channel boundaries can deeply affect the fluid flow behavior which is accentuated in curved sections.

7. References

Armani D, Liu C and Aluru N (1999), "*Re-configurable Fluid Circuits by PDMS Elastomer Micromachining*" Proc. Annual International Workshop on Micro Electro Mechanical Systems, Orlando, Florida 17-21 January 222-227.

Baart P, Green T, Li J, Lundström T S, Westerberg L G, Höglund E and Lugt P (2011), "*The influence of speed, grease type, and temperature on radial contaminant particle migration in a double restriction seal*" Trib. Trans. 54 867-877.

Bonyar A, Santha H, Ring B, Varga M, Kovacs J G and Harsanyi G (2010), "*3D Rapid Prototyping Technology (RPT) as a powerful tool in microfluidic development*" Proc. Eng. 5 291–294

Bonyár A, Sántha H, Varga M, Ring B, Vitéz A and Harsányi G (2012), "*Characterization of rapid PDMS casting technique utilizing molding forms fabricated by 3D rapid prototyping*" Int. J. Mater. Form. doi: 10.1007/s12289-012-1119-2

Brittain S, Paul K, Zhao X M and Whitesides G. M (1998), "*Soft lithography and microfabrication"* Physics World May 13 1998 31-36.

Ciftlik A T and Gijs M A M (2012), "*Parylene to silicon nitride bonding for post-integration of high pressure microfluidics to CMOS devices*" Lab Chip 12 396-400.

Egham W EP (2006), "*High pressure lubricant pump for steelworks*". European Patent EP1914425B1.

Green T, Baart P, Westerberg L G, Lundström T S, Höglund E, Lugt P and Li J (2011), "*A new method to visualize grease flow in a double restriction seal using microparticle image velocimetry*" Trib. Trans. 54 784-792.

Hardy B S, Uechi K, Zhen J and Kavehpour H P (2009), "*The deformation of flexible PDMS microchannels under a pressure driven flow*" Lab Chip 9 935-938.

Inglis D W (2010), "*A method for reducing pressure-induced deformation in silicone microfluidics*" Biomicrofluidics 4 026504 doi: 10.1063/1.3431715.

Lewpiriyawong N and Yang C (2008), "*Dielectrophoretic manipulation of particles in a modified microfluidic H filter with multi-insulating blocks*" Biomicrofluidics 2 034105.

Li J, Höglund E, Westerberg L G, Green T, Lundström T S, Lugt P M and Baart P (2012), "*μPIV measurement of grease velocity profiles in channels with two different types of flow restrictions*" Trib. Int. 54 94–99.

Li J, Westerberg L G, Höglund E, Lundström T S, Baart P, Lugt P (2013), "*Lubricating grease shear flow and boundary layers in a concentric cylinder configuration*" Proc. 3rd International Tribology Symposium of IFoMM (International Federation for the Promotion of Mechanism and Machine Science), Luleå, 19-21March 2013.

Madadi H, Mohammadi M, Casals Terré J and Castilla López R (2013), "*A novel fabrication technique to minimize PDMS-microchannels deformation under high-pressure operation*" Electrophoresis 4(22-23), 3126–3132 doi: 10.1002/elps.201300340.

Sanchez J, Rudyk S and Spirov P (2013), "*Removal of Grease from Wind Turbine Bearings by Supercritical Carbon Dioxide*" Chem. Eng. Trans. 32 1909-1914.

Stanislas M, Okamoto K and Kähler C (2003) "*Main results of the First International PIV Challenge*" Measure. Sci. Tech. 14 R63–R89.

Sultan M A, Fonte C P, Dias M, Lopes J C B and Santos J R (2012), "*Experimental study of flow regime and mixing in T-jets mixers*" Chem. Eng. Sci. 73 388-399.

Gervais Thomas, El-Ali Jamil, Günther Axel and Jensen Klavs F. (2006). "*Flow-induced of shallow microfluidic channels"* Lab Chip 6(4), 500-507, doi: 10.1039/b513524a.

Weibel D B, DiLuzio W R and Whitesides G. M (2007), "Microfabrication meets microbiology" Nature 5 209-218.

Westerberg L G, Lundström T S, Höglund E and Lugt P (2010), "*Investigation of grease flow in a rectangular channel including wall slip effects using micro particle image velocimetry"* Trib. Trans. 53 600-609.

Wu Willie, DeConinck Adam, and Lewis Jennifer A. (2011), "*Omnidirectional Printing of 3D Microvascular Networks*" Advanced healthcare materials 23 178-183.

Delo Technical Information. (2012). "Delo-photobond GB368 Technical Information", available at http://www.syneo.net/pdf/Colle/PB/colle-acrylate-uv-verre-DELO-PHOTOBOND_GB368_%28TIDB-GB%29.pdf (accessed 15 May 2014).